ACS APPLIED MATERIALS & INTERFACES

Research Article

www.acsami.org

Phosphine-Free Synthesis from 1D Pb(OH)Cl Nanowires to 0D and 1D PbSe Nanocrystals

Huaibin Shen,[†] Jinjie Li,[†] Hangying Shang,[†] Jinzhong Niu,[†] Weiwei Xu,[†] Hongzhe Wang,[†] Fang Guo,*[,‡] and Lin Song Li*[,†]

[†]Key Laboratory for Special Functional Materials of Ministry of Education, Henan University, Kaifeng 475004, China

[‡]College of Chemistry, Liaoning University, Shenyang 110036, China

Supporting Information

ABSTRACT: In this paper, we report a new phosphine-free, low-cost, low-temperature colloidal method of controlled synthesis of PbSe nanocrystals in both zero-dimension (0D) and one-dimension (1D). Different from the widely used "hot injection" method and "nonprecursor injection" method, the novelty of this new method is that it does not require a nucleation process. Instead, high-quality presynthesized 1D Pb(OH)Cl nanowires (~80 to ~160 nm in diameter) can be directly used as a Pb precursor and reacted with a Se precursor to form monodisperse dot-shaped 0D cubic PbSe and 1D orthorhombic PbSe nanowires. 0D cubic PbSe nanocrystals begin to form at elevated temperatures after the Se precursor is added to react with Pb(OH)Cl nanowires. By prolonging the reaction time for 3 h, good self-assembled 0D cubic PbSe nanocrystals can be synthesized with an average diameter of about 15 nm. Furthermore, such method has been demonstrated to synthsize high-quality 1D PbSe nanowires successfully with temperature as low as 110 °C. 1D PbSe nanowires possess a mean diameter of 15−24 nm with the shortest and longest length from 600 nm to 5 μm. The only sharp and strong peak, which is consistent with characteristic peaks of orthorhombic PbSe, indicates that the nanowires' elongation axis is in the [111] direction, and 0D cubic PbSe nanocrystals change to 1D orthorhombic PbSe nanowires completely.

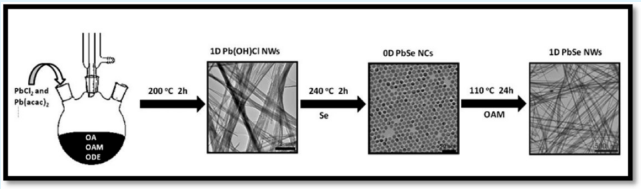

KEYWORDS: *Pb(OH)Cl, PbSe, nanocrystals, nanowires, colloidal method*

1. INTRODUCTION

Among various nanomaterials, synthesis of zero-dimensional (0D) and one-dimensional (1D) building blocks (such as quantum dots for 0D, nanorods and nanowires for 1D) has attracted intense research interest due to the presence of carrier confinement in these nanomaterials combined with tunable geometry and the attendant novel optoelectronic properties, and thereafter, such materials potentially contribute to a wide range of applications.[1−7] In fact, the future of 0D and 1D nanoscale building blocks will be largely dependent on how well we can balance the issues of cost, performance, and stability of such building block-based devices and systems. Therefore, it is very important to exploit reliable and reproducible new methods for producing large-scale, uniformly sized 0D and 1D nanoscale building blocks.

Recently, lead chalcogenide nanostructures have been extensively studied due to their prospective applications in photodetectors, solar cells, light-emitting diodes, and biolabeling, etc.[8−12] Up to now, many approaches have been explored for the synthesis of 0D and 1D lead chalcogenide nanomaterials, such as solution-based methods,[11,13−16] chemical vapor deposition (CVD),[17−19] vapor−liquid−solid methods,[20,21] and electrodeposition.[22,23] Here, we report a new phosphine-free, low-cost, low-temperature colloidal method for controlled synthesis of PbSe nanocrystals in both 0D and 1D. Different from the widely used "hot injection" method[24] and "nonprecursor injection" method,[5] the novelty of this new method does not require a nucleation process. Instead, high-quality presyntheiszed 1D Pb(OH)Cl nanowires can be directly used as a Pb precursor and reacted with the Se precursor to form monodisperse dot-shaped 0D PbSe nanocrystals. After further overnight annealing at a low temperature, 0D PbSe nanocrystals have been eventually changed to 1D PbSe nanowires successfully (Scheme 1). The unique point of this synthesis method is a "fast" nucleation that has been skipped, and high-quality 0D and 1D PbSe nanocrystals can undergo controlled synthesis within a relatively slow reaction time (2 to 24 h) compared to the ultrafast reaction speed (several seconds to minutes) for the traditional "high-temperature injection for nucleation and low-temperature for growth" method. Such a slow reaction speed not only facilitates to adjust the reaction conditions and obtain different sizes and shapes of nanocrystals but also takes advantage of the design of some complicated synthesis for doping, alloy, and core/shell etc.

Received: August 12, 2013
Accepted: September 25, 2013
Published: September 25, 2013

Scheme 1. Synthetic Procedure for Pb(OH)Cl Nanowires, 0D Dot-Shaped PbSe Nanocrystals, and 1D PbSe Nanowires

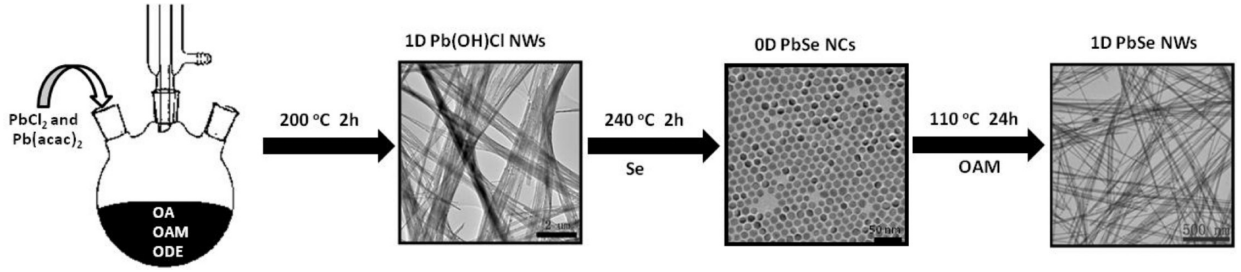

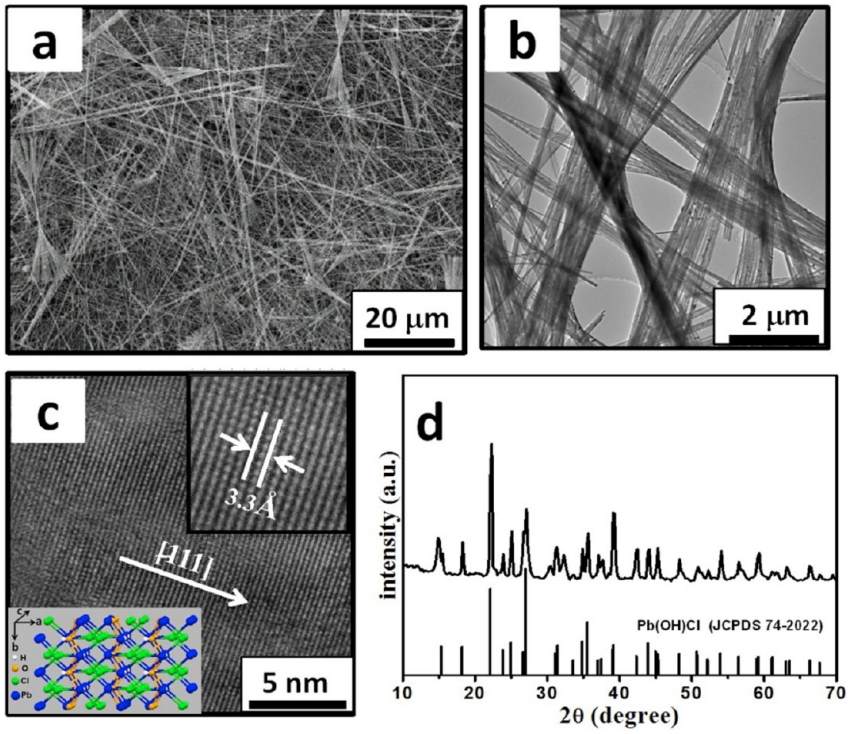

Figure 1. Characterization of 1D Pb(OH)Cl nanowires prepared by the solution method: (a) SEM image; (b) TEM image; (c) high-resolution TEM (HRTEM) image (inset: atomistic model of the crystal structure); (d) X-ray diffraction (XRD) pattern. The vertical bars represent the standard XRD patterns of orthorhombic structure Pb(OH)Cl.

2. EXPERIMENTAL SECTION

Chemicals. Oleic acid (OA, 90%), oleylamine (OAM, 70%), selenium (Se, 99.99%, powder), and 1-octadecene (ODE, 90%) were purchased from Aldrich. Hexanes (analytical grade), acetone (analytical grade), chloroform (analytical grade), ethanol (analytical grade), lead chlorides ($PbCl_2$, analytical reagent), acetylacetone (acac, 99.5%), and triethylamine (99.0%) were obtained from Beijing Chemical Reagent Ltd., China. All reagents were used as received without further experimental purification.

Synthesis of Lead Acetylacetonates [Pb(acac)$_2$]. In a typical synthesis, 20 mmol of $PbCl_2$ was dissolved in 10 mL of deionized water. Under magnetic stirring, acetylacetone (5 mL, 50 mmol) was added and kept stirring for 15 min. $Pb(acac)_2$ was precipitated after an appropriate amount of triethylamine was added in the solution. Then, $Pb(acac)_2$ was washed 3 times with ethanol (50 mL each time) and water (50 mL each time). Finally it was dried in vacuum at 50 °C for further use.

Stock Solutions for Se Precursors. Amounts of 0.1185 g (1.5 mmol) of Se powder and 15 mL of ODE were added together in a three-neck flask, then heated to 280 °C under nitrogen flow for 3 h until the solution became a clear yellow color, and then cooled to room temperature for further use.

Synthesis of Pb(OH)Cl Nanowires. $Pb(acac)_2$ (0.081 g, 0.2 mmol), $PbCl_2$ (0.11 g, 0.4 mmol), 0.4 mmol of OA, and 0.4 mmol of OAM were added to ODE (5 mL) in a three-necked flash. The reaction mixture was heated to 200 °C and maintained for 2 h under stirring and nitrogen flow. A white product (Pb(OH)Cl nanowires) was formed gradually.

Synthesis of PbSe Nanocrystals. An amount of 6 mL of Se precursor (0.6 mmol) stock solution was added to Pb(OH)Cl precursor (0.2 mmol) in a three-necked flask. Then it was heated to 240 °C and maintained at that temperature for 3 h. After reaction, it was cooled to room temperature naturally. The product was precipitated by introducing acetone and centrifuging at 4000 rpm. The precipitate was washed three times with acetone and dried at 50 °C. The as-obtained nanocrystals can be redispersed into nonpolar solvents such as hexanes or toluene.

Synthesis of PbSe Nanowires. The purified PbSe nanocrystals in hexanes and 6 mL of OAM were added into a three-necked flask, and the system was kept at 75 °C under nitrogen flow for 30 min to remove hexanes with low vapor pressure. Subsequently, the solution was heated to 110 °C for 24 h. The product was precipitated by introducing acetone and centrifuging at 4000 rpm.

Characterization. Scanning electron microscope (SEM) studies were preformed on a JSM-5600LV. Transmission electron microscopy (TEM) and high-resolution transmission electron microscopy

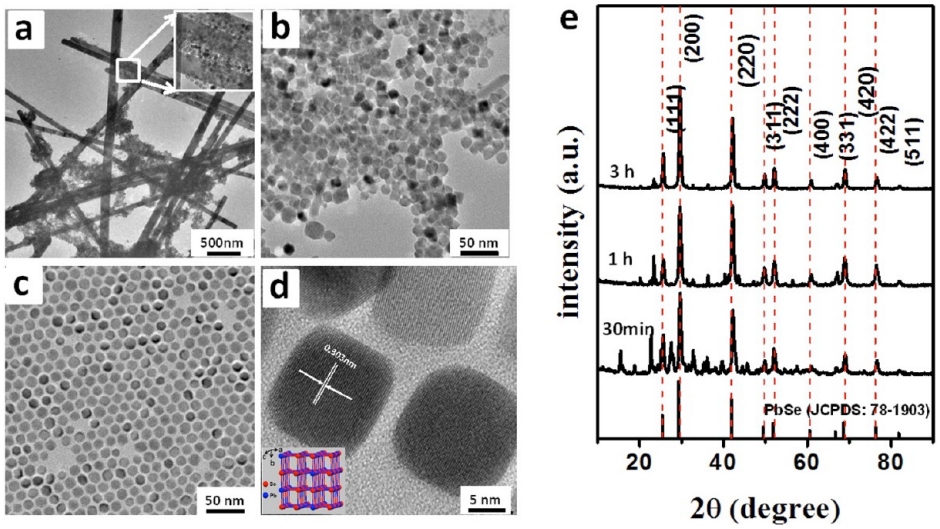

Figure 2. Evolution of TEM images of 1D Pb(OH)Cl nanowires changes to 0D PbSe nanocrystals, and reaction time lasted (a) 30 min, (b) 1 h, and (c) 3 h. (d) High-resolution TEM image of Figure 2c (inset: atomistic model of the crystal structure). (e) Corresponding XRD patterns of a, b, and c. The vertical bars represent the standard XRD patterns of cubic structure PbSe.

(HRTEM) observations were performed with a JEOL JEM-2010 microscope with an accelerating voltage of 200 kV. Phase determination of the products was carried out by a Philips X'Pert Pro X-ray diffractometer (XRD) using Cu Kα radiation (λ = 1.54 Å).

3. RESULTS AND DISCUSSION

Pb(OH)Cl nanowires were synthesized successfully by simply controlling the molar ratios of $PbCl_2$/$Pb(acac)_2$. To observe the morphology of as-prepared Pb(OH)Cl nanowires, SEM and TEM analyses were carried out. Figure 1 and Figure S1 (Supporting Information) show SEM and TEM images of Pb(OH)Cl nanowires which were prepared at 200 °C with the molar ratio of $PbCl_2$/$Pb(acac)_2$ = 2:1. TEM images of Pb(OH)Cl nanowires synthesized with different molar ratios of $PbCl_2$/$Pb(acac)_2$ and different temperatures are shown in Figure S2 and Figure S3 (Supporting Information), respectively. The quality of Pb(OH)Cl nanowires depends on the molar ratios of $PbCl_2$/$Pb(acac)_2$ and reaction temperature. The as-prepared 1D Pb(OH)Cl nanowires were nearly defect-free with uniform diameter along the entire length. The wires' dimensions could be tuned from ~80 to ~160 nm in diameter, and lengths up to hundreds of micrometers were obtained by tailoring reaction conditions, some of the nanowires aligning into bundles with individual nanobelts being longer than 50 μm. Figure 1c shows a high-resolution TEM (HRTEM) image of one Pb(OH)Cl nanowire. The *d*-spacing of 0.33 nm calculated from the HRTEM image indicates that the nanowires are growing along the ⟨111⟩ direction. The basis for an atomistic model of the Pb(OH)Cl nanowire along the *c* axis is shown in the insets. The X-ray diffraction (XRD) pattern from the as-prepared 1D nanowires reveals the orthorhombic crystal structure (see Figure 1d), which is consistent with the HRTEM result.

Figure 2 shows the process of 1D Pb(OH)Cl nanowires changed to 0D PbSe nanocrystals. Once 1D Pb(OH)Cl nanowires were synthesized, the Se precursor was added to react with Pb(OH)Cl nanowires. 0D PbSe nanocrystals began to form at elevated temperatures. When the reaction time only lasted 30 min after adding the Se precursor, the 0D PbSe nanocrystals began to form (Figure 2a). It is a coexistence of 1D Pb(OH)Cl nanowires and 0D PbSe nanocrystals. 1D Pb(OH)Cl nanowires almost completely changed into 0D PbSe nanocrystals after the reaction lasted for 1 h, but the size of the PbSe nanocrystals was not homogeneous at this moment (Figure 2b). By prolonging the reaction time for another 2 h, good self-assembled 0D PbSe nanocrystals can be synthesized with an average diameter of about 15 nm (Figure 2c). The HRTEM image shown in Figure 2d indicates that the distances between the adjacent lattice fringes are ~0.3 nm, in accordance with the interplanar distances of the (200) plane of cubic phased PbSe.[25,26] To further characterize the evolution of structures from 1D Pb(OH)Cl nanowires to 0D PbSe nanocrystals, their crystallographic properties were determined by XRD (Figure 2e). According to the XRD pattern, the crystal changed from orthorhombic Pb(OH)Cl nanowires to cubic phase PbSe nanocrystals gradually (JCPDS, 78-1903) after adding the Se precursor. The schematic diagram of a possible mechanism for the formation of PbSe nanocrystals from Pb(OH)Cl nanowires is shown in Figure S4 (Supporting Information). We speculate that the formation of PbSe nanocrystals is the result of gradual erosion of Pb(OH)Cl nanowires and consequent growth of PbSe nanocrystals. As shown in Figure S4 (Supporting Information), the Pb(OH)Cl nanowires acted as the Pb precursor. By the ion exchange, the OH^- and Cl^- ions were stripped from the nanowires, and the wire structure of Pb(OH)Cl nanowires was destroyed. The Pb^{2+} ions reacted with Se^{2-}, and monodisperse PbSe nanocrystals were formed finally.

Different from high-temperature injection and the selenium phosphine method,[14,16,26−29] this method is a phosphine-free, low-cost colloidal method for the synthesis of high-quality 0D PbSe nanocrystals because trioctylphosphine (TOP) and tributylphosphine (TBP) are hazardous, unstable, and expensive and generally require glovebox operation. Furthermore, such a method has been further demonstrated to synthsize 1D PbSe nanowires successfully with low temperature, whereas most reports about nanowires of PbSe have been grown by a number of methods with high temperature,[17−21] although solution-based methods can give rise to good yields of NWs at low temperatures (<400 °C) but still need to be higher than 200 °C.[14,16] Here this method just needed 110 °C for the synthesis of high-quality PbSe nanowires. After the synthesis of

cubic 0D PbSe nanocrystals, they were purified and added into oleylamine and aged at 110 °C for 24 h, and 1D PbSe nanowires were synthesized. Figure 3a, b, and c shows

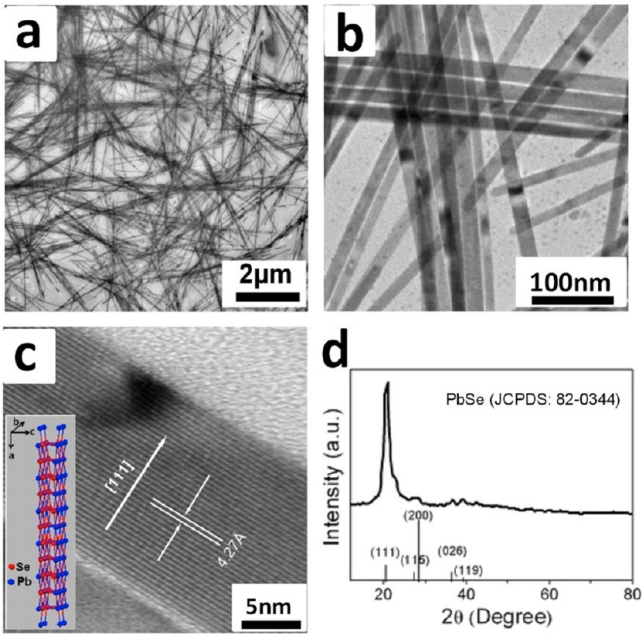

Figure 3. (a and b) Low- and high-magnification TEM images of 1D PbSe nanowires. (c) Corresponding HRTEM image of PbSe nanowires (inset: atomistic model of the crystal structure). (d) XRD pattern of PbSe nanowires. The vertical bars represent the standard XRD patterns of orthorhombic structure PbSe.

representative low- and high-resolution TEM images of the 1D PbSe nanowires. Clear lattice fringes are clearly evident to illustrate their good crystallinity. These wires also show smooth surfaces and exhibit straight morphologies, which are opposed to the branched shapes previously seen in solution-grown PbSe NWs.[13,29] As shown in Figure 3a and b, 1D PbSe nanowires possess a mean diameter of 15−24 nm (Figure S5, Supporting Information) with the shortest and longest length from 600 nm to 5 μm (Figure S6, Supporting Information). Furthermore, the HRTEM image reveals that the interplanar distance along the growth axis is 0.427 nm, which is consistent with the interplanar distance of the (111) plane of the orthorhombic structure of PbSe, thus confirming that the nanowires' elongation axis was in the [111] direction. The basis for an atomistic model of the Pb(OH)Cl nanowire along the *c* axis is shown in the inset. PbSe nanowires' structures were further characterized using XRD measurement. Figure 3d shows the XRD pattern of PbSe nanowires, and it can be seen that the only peak position located at 20.8° matched well with the (111) plane of the orthorhombic structure of PbSe, which is consistent with the HRTEM result.

To understand the formation mechanism of 1D PbSe nanowires, XRD and TEM were used to monitor the growth process dynamically. The XRD and TEM results (Figure 4a−e and f) unambiguously illustrate the following process: Almost no changes occurred after adding 0D PbSe nanocrystals into OAM for the first 10 min, 0D PbSe nanocrystals kept the same shapes from the TEM image, and there is no change of the characteristic diffraction peaks from the XRD pattern. 0D PbSe nanocrystals gradually disappeared after aging for 3 h. 1D PbSe nanowires with diameter about 5 nm and length between 20

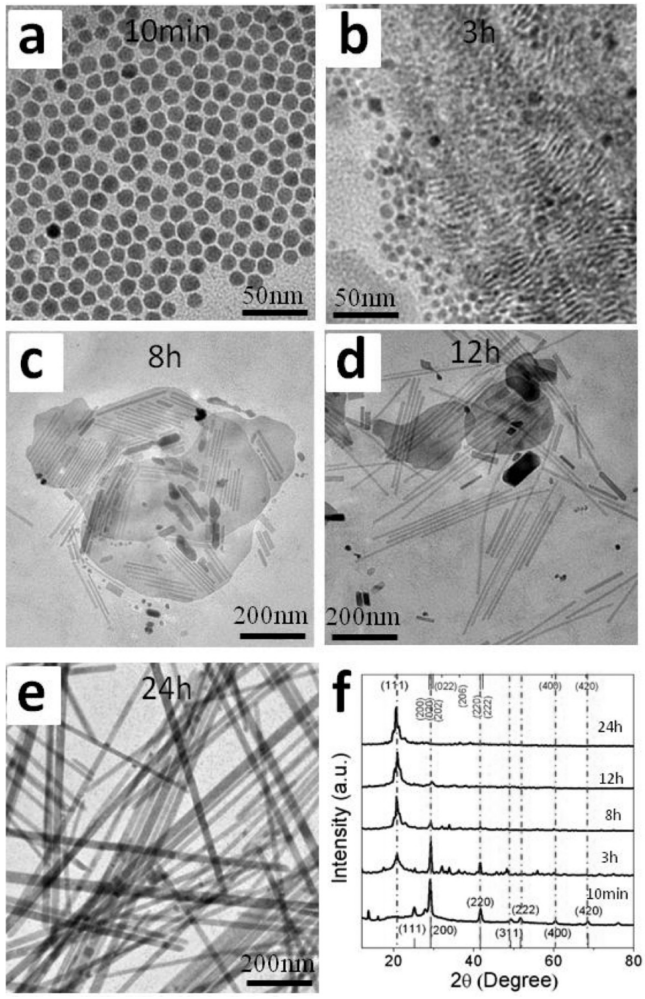

Figure 4. Evolution of 0D PbSe nanocrystals change to 1D PbSe nanowires, monitored by TEM (a−e) and XRD (f). The vertical bars represent the standard XRD patterns of cubic (bottom: JCPDS: 78-1903) and orthorhombic (top: JCPDS: 82-0344) structure PbSe.

and 100 nm began to form. In fact, the XRD diffraction peaks began to change, and a new characteristic peak located at 20.8° appeared with low intensity. The XRD data were consistent with the TEM results. 1D PbSe nanowires kept growing once the reaction solution was further aged another 8 h, and many 1D nanowires with under 200 nm length were formed. As the new peak became more evident, the peaks from cubic PbSe were gradually weakened, and some almost disappeared, which suggests the disappearance of the cubic structure of PbSe. The new peak actually matches well with the (111) plane of the orthorhombic structure of PbSe (JCPDS: 82-0344). With further aging for 12 h, the length of the PbSe nanowires slowly grew over 200 nm, and the characteristic diffraction peaks for orthorhombic PbSe nanowires were progressively enhanced.

Eventually, high yields of 1D PbSe nanowires with high uniformity and straight morphology shapes were formed after the entire reaction lasted as long as 24 h. The diameters of 1D PbSe nanowires are between 15 and 22 nm, and lengths are up to several micrometers (Figure 4 e). The characteristic peaks of cubic PbSe disappeared completely (Figure 4 f). The only sharp and strong peak, which is consistent with characteristic peaks of orthorhombic PbSe, indicates that the nanowires' elongation axis is in the [111] direction, and 0D cubic PbSe nanocrystals

change to 1D orthorhombic PbSe nanowires completely. Such a transformation from cubic to orthorhombic structure monitored by XRD and TEM can be explained by the cubic system of 0D PbSe nanocrystals transformed by forming a superstructure along the *c*-axis (corresponding to a quadrupled unit cell repeated in this direction), together with a distortion in the ab plane, resulting in an orthorhombic structure of 1D PbSe nanowires.

To clarify the roles of surface ligands in the transformation from 0D PbSe nanocrystals to 1D PbSe nanowires, FTIR spectra were measured, and the results are shown in Figure S7 (Supporting Information). For the PbSe nanocrystals and nanowires, the vibration bands are located at 2956, 1644, and 1486 cm^{-1} and other characteristic IR bands which are identical with the FTIR spectrum of OAM. No bands were found to be located at 1711 cm^{-1}, which are the characteristic IR bands for OA. This means OAM is the only ligand for PbSe nanocrystals, and the solvent used here is also OAM. So OAM played an important role in the transformation from the PbSe nanocrystals to nanowires. The mechanism for shape-controlled synthesis is based on the kinetics control in the growth process by binding surfactants onto different crystal facets.[15] Therefore, such surfactant binding leads to a decrease or increase in crystal growth rate at different facets. Here OAM not only played as surfactant and solvent but also acted as a ligand to form stable complexes with Pb and Se on the surface of PbSe nanocrystals (Figure 4b and Figure S8, Supporting Information). When the concentration of Pb-OAM and Se-OAM was high enough to induce the renucleation, the formation of PbSe nanorods is observed during the aging of colloidal solutions of PbSe nanocrystals (Figure 4c and Figure S8, Supporting Information). With the existence of extra OAM, the preferential growth of (111) facets is observed. By the oriented growth of Pb-OAM and Se-OAM, 1D PbSe nanowires are formed. The schematic diagram of the proposed mechanism for the formation of PbSe nanowires is shown in Figure S8 (Supporting Information). We think the PbSe nanowire is formed by the selective adhesion of precursors on the (111) facets. To explore the universality of this method, we synthesized cube (Figure S9a, Supporting Information) shaped PbSe nanocrystals using the phosphine-contained method,[30] and then we adopted the same method and tried to obtain 1D PbSe nanowires. However, there were no 1D PbSe nanowires formed, and only very short rods were observed (Figure S9b, Supporting Information).

4. CONCLUSION

In summary, we report a robust method for controlled synthesis of high-quality 1D Pb(OH)Cl nanowires which can be used to synthesize 0D PbSe nanocrystals and 1D PbSe nanowires via a phosphine-free, low-cost, low-temperature colloidal method. It is a new finding that no nucleation process is really needed to synthesis high-quality 0D and 1D nanocrystals. Thereafter, this method demonstrates not only 1D nanowires can be used as a precursor to synthesize 0D nanocrystals but also 0D nanocrystals can be used to grow 1D nanowires successfully. With the methodology of constructing 0D and 1D PbSe reported in this communication, we believe that it may turn a new leaf of manipulation of 0D and 1D nanoscale building blocks and many related potential applications.

■ ASSOCIATED CONTENT

Supporting Information

TEM images of Pb(OH)Cl nanowires, schematic diagram of the synthetic route and proposed mechanism for the formation of PbSe nanocrystals from Pb(OH)Cl nanowires and PbSe nanowires from PbSe nanocrystals, TEM images of PbSe nanocrystals and nanowires, and FTIR of PbSe nanocrystals and PbSe nanowires. This material is available free of charge via the Internet at http://pubs.acs.org.

■ AUTHOR INFORMATION

Corresponding Authors

*E-mail: lsli@henu.edu.cn.
*E-mail: fguo@lnu.edu.cn.

Notes

The authors declare no competing financial interest.

■ ACKNOWLEDGMENTS

This work was financially supported by the research project of the National Natural Science Foundation of China (21071041 and 21201055), Program for Changjiang Scholars and Innovative Research Team in University, (No. PCS IRT1126), and Program for New Century Excellent Talents in University of Chinese Ministry of Education (NCET-09-0119).

■ REFERENCES

(1) Alivisatos, A. P. *Science* **1996**, *271*, 933−937.
(2) Murray, C. B.; Kagan, C. R.; Bawendi, M. G. *Annu. Rev. Mater. Sci.* **2000**, *30*, 545−610.
(3) Huang, Y.; Duan, X. F.; Cui, Y.; Lauhon, L. J.; Kim, K. H.; Lieber, C. M. *Science* **2001**, *294*, 1313−1317.
(4) (a) Sigman, M. B.; Korgel, B. A. *J. Am. Chem. Soc.* **2005**, *127*, 10089−10095. (b) Dong, A.; Yu, H.; Wang, F.; Buhro, W. E. *J. Am. Chem. Soc.* **2008**, *130*, 5954−5961. (c) Wang, F.; Yu, H.; Li, J.; Hang, Q.; Zemlyanov, D.; Gibbons, P. C.; Wang, L.-W.; Janes, D. B.; Buhro, W. E. *J. Am. Chem. Soc.* **2007**, *129*, 14327−14335. (d) Sun, J.; Buhro, W. E. *Angew. Chem., Int. Ed.* **2008**, *120*, 3259−3262.
(5) (a) Mandal, S.; Mandal, A.; Banerjee, S. *ACS Appl. Mater. Interfaces* **2012**, *4*, 205−209. (b) Etgar, L.; Park, J.; Barolo, C.; Nazeeruddin, M.; Viscardi, G.; Graetzel, M. *ACS Appl. Mater. Interfaces* **2011**, *3*, 3264−3267. (c) Yu, K.; Ouyang, J.; Leek, D. *Small* **2011**, *7*, 2250−2262.
(6) Yin, Y.; Alivisatos, A. P. *Nature* **2005**, *437*, 664−670.
(7) Zhu, G.; Xu, Z. *J. Am. Chem. Soc.* **2011**, *133*, 148−157.
(8) (a) Sun, L.; Choi, J. J.; Stachnik, D.; Bartnik, A. C.; Hyun, B. R.; Malliaras, G. G.; Hanrath, T.; Wise, F. W. *Nat. Nanotechnol.* **2012**, *7*, 369−373. (b) Konstantatos, G.; Howard, I.; Fischer, A.; Hoogland, S.; Clifford, J.; Klem, E.; Levina, L.; Sargent, E. H. *Nature* **2006**, *442*, 180−183.
(9) (a) Dai, Q.; Wang, Y.; Li, X.; Zhang, Y.; Pellegrino, J.; Zhao, M.; Zou, B.; Seo, J.; Wang, Y.; Yu, W. W. *ACS Nano* **2009**, *3*, 1518−1524. (b) Moreels, I.; Lambert, K.; Muynck, D. D.; Vanhaecke, F.; Poelman, D.; Martins, J. C.; Allan, G.; Hens, Z. *Chem. Mater.* **2007**, *19*, 6101−6106. (c) Onicha, A. C.; Petchsang, N.; Kosel, T. H.; Kuno, M. *ACS Nano* **2012**, *6*, 2833−2838. (d) Hanrath, T.; Veldman, D.; Choi, J.; Christova, C.; Wienk, M.; Janssen, R. *ACS Appl. Mater. Interfaces* **2009**, *1*, 244−250.
(10) (a) Sargent, E. H. *Adv. Mater.* **2008**, *20*, 3958−3964. (b) Sarasqueta, G.; Choudhury, K. R.; So, F. *Chem. Mater.* **2010**, *22*, 3496−3501. (c) Ma, W.; Luther, J. M.; Zheng, H.; Wu, Y.; Alivisatos, A. P. *Nano Lett.* **2009**, *9*, 1699−1703. (d) Zhao, N.; Osedach, T. P.; Chang, L. Y.; Geyer, S. M.; Wanger, D.; Binda, M. T.; Arango, A. C.; Bawendi, M. G.; Bulovic, V. *ACS Nano* **2010**, *4*, 3743−3752. (e) Choi, J. H.; Chen, K. H.; Strano, M. S. *J. Am. Chem. Soc.* **2006**, *128*, 15584−15585.

(11) (a) Wu, X. J.; Zhu, F.; Mu, C.; Liang, Y.; Xu, L.; Chen, Q.; Chen, R.; Xu, D. *Coord. Chem. Rev.* **2010**, *254*, 1135−1150. (b) Ouyang, J.; Schuurmans, C.; Zhang, Y.; Nagelkerke, R.; Wu, X.; Kingston, D.; Wang, Z.; Wilkinson, D.; Li, Ch; Leek, D.; Tao, Y.; Yu, K. *ACS Appl. Mater. Interfaces* **2011**, *3*, 553−565. (c) Yu, K.; Ouyang, J.; Zhang, Y.; Tung, H.; Lin, S.; Nagelkerke, R.; Kingston, D.; Wu, X.; Leek, D.; Wilkinson, D.; Li, C.; Chen, I.; Tao, Ye. *ACS Appl. Mater. Interfaces* **2011**, *3*, 1511−1520.
(12) Hujdic, J. E.; Taggart, D. K.; Kung, S. C.; Menke, E. J. *J. Phys. Chem. Lett.* **2010**, *1*, 1055−1059.
(13) Akhtar, J.; Akhtar, M.; Malik, M. A.; Brien, P.; Raftery, J. *J. Am. Chem. Soc.* **2012**, *134*, 2485−2487.
(14) Koh, W. K.; Bartnik, A. C.; Wise, F. W.; Murray, C. B. *J. Am. Chem. Soc.* **2010**, *132*, 3909−3913.
(15) Mokari, T.; Zhang, M.; Yang, P. *J. Am. Chem. Soc.* **2007**, *129*, 9864−9865.
(16) Mokari, T.; Habas, S. E.; Zhang, M.; Yang, P. *Angew. Chem., Int. Ed.* **2008**, *47*, 5605−5608.
(17) Matthew, J. B.; Lau, Y. K. A.; Kvit, A. V.; Schmitt, A. L.; Jin, S. *Science* **2008**, *320*, 1060−1063.
(18) Bierman, M. J.; Lau, Y. K. A.; Jin, S. *Nano Lett.* **2007**, *7*, 2907−2912.
(19) Lau, Y. K. A.; Chernak, D. J.; Bierman, M. J.; Jin, S. *J. Am. Chem. Soc.* **2009**, *131*, 16461−16471.
(20) Zhu, J.; Peng, H.; Chan, C. K.; Jarausch, K.; Zhang, X. F.; Cui, Y. *Nano Lett.* **2007**, *7*, 1095−1099.
(21) Dziawa, P.; Sadowski, J.; Dluzewski, P.; Lusakowska, E.; Domukhovski, V.; Taliashvili, B.; Wojciechowski, T.; Baczewski, L. T.; Bukala, M.; Galicka, M.; Buczko, R.; Kacman, P. T. *Cryst. Growth Des.* **2010**, *10*, 109−113.
(22) Nişanc, F. B.; Demir, U. *Langmuir* **2012**, *28*, 8571−8578.
(23) Yang, Y.; Kung, S. C.; Taggart, D. K.; Xiang, C.; Yang, F.; Brown, M. A.; Güell, A. G.; Kruse, T. J.; Hemminger, J. C.; Penner, R. M. *Nano Lett.* **2008**, *8*, 2447−2451.
(24) Murray, C. B.; Norris, D. J.; Bawendi, M. G. *J. Am. Chem. Soc.* **1993**, *115*, 8706−8715.
(25) Xu, J.; Ge, J.; Li, Y.-D. *J. Phys. Chem. B* **2006**, *110*, 2497−2501.
(26) Yu, W. W.; Falkner, J. C.; Shih, B. S.; Colvin, V. L. *Chem. Mater.* **2004**, *16*, 3318−3322.
(27) Yong, K.-T.; Sahoo, Y.; Choudhury, K.; Swihart, M.; Minter, J. R.; Prasad, P. *Nano Lett.* **2006**, *6*, 709−714.
(28) Cho, K. S.; Talapin, D. V.; Gaschler, W.; Murray, C. B. *J. Am. Chem. Soc.* **2005**, *127*, 7140−7147.
(29) Hull, K. L.; Grebinski, J. W.; Kosel, T. H.; Kuno, M. *Chem. Mater.* **2005**, *17*, 4416−4425.
(30) Lu, W. G.; Fang, J. Y.; Ding, Y.; Wang, Z. L. *J. Phys. Chem. B* **2005**, *109*, 19219−19222.